SEMINAR: COMPUTATIONAL METHODS FOR IMAGE RECONSTRUCTION (FINAL REPORT

Chapter 3: Analytical Tomographic Image Reconstruction Methods

BOEY KAI ZHE[1]

CONTENTS

1 INTRODUCTION

The 3 common types of computer tomography (CT) geometries are parallel beam, fan beam, and cone beam. Developed in 1971, parallel beam geometry or 1st generation CT *(Figure 1 left)* was the first to allow the cross-section of an object to be imaged. The X-ray source and detectors are aligned parallel to each other during rotation around the patient, creating a set of parallel rays. Its downside is that it's extremely slow and takes approximately 5 minutes to acquire 1 projection image.

An improvement of the original parallel beam CT was invented in 1975 and was known as the fan beam CT or 3rd generation CT *(Figure 1 center)*. This configuration involves a collimated X-ray beam that diverges from the X-ray source to create a fan-shaped radiation pattern. As the X-ray source and detectors rotate around the patient, the fan beam captures data from multiple angles. Like the parallel beam CT, it allows 2D cross-sectional images to be reconstructed from projections. A major improvement is the time to acquire projection images is shortened considerably.

The cone beam geometry *(Figure 1 right)*, part of the third generation of CT, shares a same principle with fan beam CT but it can reconstruct 3D cross-sectional images. This involves using a 2 dimensional detector rather that a 1 dimension detector in the previous two geometries. Cone beam CT stands out for its rapid acquisition of projection images, even surpassing fan beam CT.

This report focuses only on the fan beam (section 2) and cone beam CT (section 3). The geometrical properties and forward projection process to acquire projection images will be explained briskly. Nevertheless, the main focus will be on the reconstruction process where various algorithms are discussed in detail and results from my own implementation are used to illustrate the algorithm further.

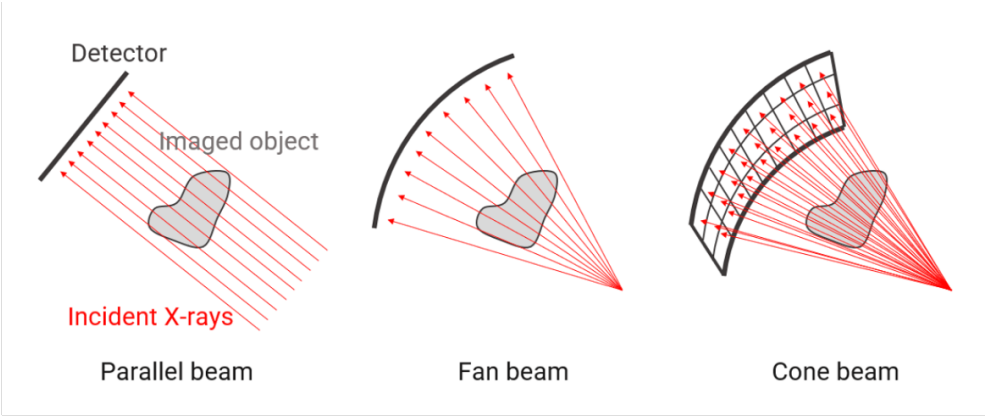

Figure 1: Fan beam geometry, source: https://imaging.rigaku.com/blog/how-does-ct-reconstruction-work

2 2D FAN BEAM TOMOGRAPHY

Various reconstruction methods are explored, including rebinning from fan-beam to parallel-beam measurements, filtered back projections, and backprojection filters, which will be discussed in subsequent sections. However, a comprehensive understanding of the underlying geometries and parameters is essential and will be thoroughly addressed before delving into the reconstruction algorithms. Note that this report follows the chapter structure in the book[1], placing the filter-backprojection method after the fan parallel rebinning method, even though the order is reversed in the slide.

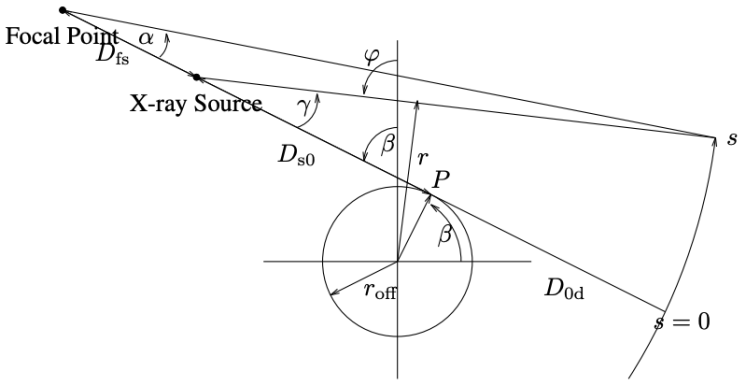

Figure 2: Fan beam geometry, source: [1]

Figure 2 illustrates the geometry of fan-beam geometries. Let the focal point, X-ray source, center of rotation, and detector be denoted by f, s, o, and d respectively. A line between the X-ray source and detector passes through the center of rotation, and an offset r_{off} is to account for the mismatched distance between this line and the center. Then, let P denote the point along that line that intersects the circle of radius r_{off} at the rotation isocenter. Some important distance parameters

are D_{fs} - the distance from the focal point f to the X-ray source s; D_{so} - distance from the X-ray source s to P; D_{od} - distance from p to the center of detector d; $D_{sd} = D_{od} + D_{so}$ - total distance from the X-ray source to the center of the detector; and $s \in [-s_{max}, s_{max}]$ - arc length along the detector. Important angular parameters are β - angle that the line segment between the X-ray source and the detector center makes with the y axis.

It is important to distinguish the 2 important fan-beam geometries which are the equiangular and equidistant case as they lead to some differences in the reconstruction algorithm. The former utilizes a curved detector while the latter utilizes a flat detector. Furthermore, $D_{fs} = 0$ for curved detector and $D_{fs} = \infty$ for flat detector. The use of different detectors leads to a different relationship for γ as shown in the following equations:

$$\gamma(s) = \begin{cases} \frac{s}{D_{sd}}, & \text{if } D_{fs} = 0 \text{ (equiangular)} \\ \arctan(\frac{s}{D_{sd}}), & \text{if } D_{fs} = \infty \text{ (equidistant)} \end{cases} \tag{1}$$

$$s(\gamma) = \gamma^{-1}(s) = \begin{cases} D_{sd}\gamma, & \text{if } D_{fs} = 0 \text{ (equiangular)} \\ D_{fd}[\gamma - \arcsin(\frac{D_{fs}}{D_{fd}} \sin\gamma)], & \text{if } 0 \leqslant D_{fs} \leqslant \infty \\ D_{sd} \tan\gamma, & \text{if } D_{fs} = \infty \text{ (equidistant)} \end{cases} \tag{2}$$

Moreover, let $L(s, \beta) = \{(x, y) : x \cos\phi(s, \beta) + y \sin\phi(s, \beta) = r(s)\}$ denotes the ray corresponding to angle β and detector element s; $\gamma_{max} = \gamma(s_{max})$ and s_{max} is half of the total arc length of the detector; r_{max} denotes the circular field of view of the imaging system; and the angle $2\gamma_{max}$ denotes the fan angle. Then, we have the relationship: $|r(s)| \leqslant r_{max} = D_{s0} \sin\gamma_{max}$

Similar to the parallel beam projection, the fan-beam projection is a collection of line integrals that passes through a 2D object f(x,y) at each rotation angle but is parameterized in terms of the variables β and s instead of r and ϕ in the parallel beam case. Let the projection be defined as:

$$p(s, \beta) = \int_{L(s,\beta)} f(x, y)\, d\ell = \iint f(x, y)\delta(x \cos\phi(s.\beta) + y \sin\phi(s.\beta) - r(s))\, dx\, dy \tag{3}$$

The goal of the reconstruction is to estimate f(x,y) from equation (3) by estimating the attenuations of X-ray in the object. The aforementioned parameters above and their relationships play a vital role in deriving the reconstruction algorithm in the subsequent section.

Now, a demonstration of the fan-beam projection will be made. Given a test phantom image as f(x,y), and using the geometrical setup for the equidistant case - (i) 420 projections; (ii) arc/ γ = 360; (iii) distance from the X-ray source to P/ D_{so} = 12800; (iv) distance from P to detector / D_{od} = 128; (v) offset = 0; (vi) Size of the detector/ s = 180; (vii) Sino and volume spacing = 1 (unit spacing); (viii) Joseph projection method, the resulting forward projection of the test phantom defined in equation (3) is shown in figure 3 below:

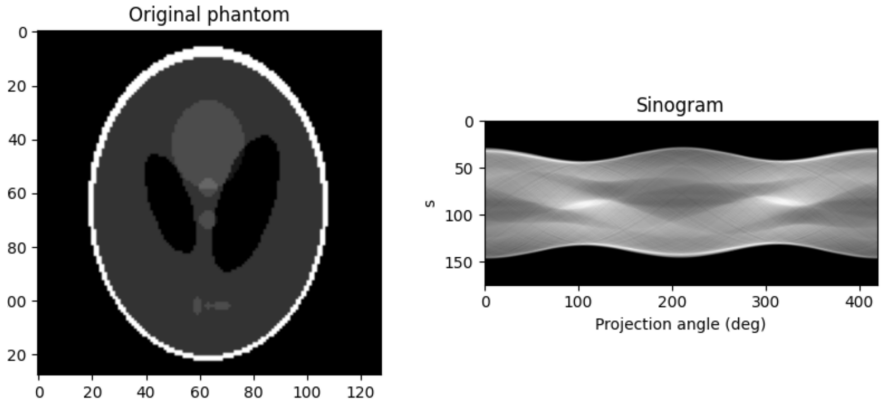

Figure 3: Test phantom (left) and resulting sinogram (right) created using the geometrical setup

2.1 Fan-parallel rebinning methods

Rebinning is a method to transform the fan-beam projections into parallel-beam projections by finding equal rays in both geometries. The idea behind is to express the fan beam projection in equation (3) in terms of parallel-beam projections. This is done by expressing s and β in terms of the parallel-beam parameters r and ϕ. By applying a change in variable and choosing $\phi = \beta + \gamma$ and $r = D_{s0} \sin\gamma$ [2], equation (3) can be written as:

$$p_\phi(r) = p(s,\beta)|_{s=s(r),\beta=\beta(r,\phi)} = p(\gamma^{-1}(\arcsin r/D_{so}, \phi - \arcsin r/D_{so})) \quad (4)$$

Next, the rebinning is achieved using 2 interpolation since there are 2 change of variables. The 2 interpolations are: (i) angular interpolation - 1D interpolation along the source position using the relationship $\phi = \beta + \gamma$; and (ii) radial interpolation - 1D interpolation along the detector using the relationship $r = D_{so} \sin\gamma$.

In *Figure 4*, the process begins with applying the Radon transform to a test phantom, yielding a parallel-beam sinogram *(fig. 4 left)*. Using the para2fan method in Matlab, the sinogram is rebinned into a fan-beam format *(fig. 4 centre)*. Subsequently, the fan2para method is employed to rebin the fan-beam sinogram back to a parallel-beam configuration *(fig. 4 right)*. The mean squared error between the original fan beam sinogram and the rebinned parallel-beam sinogram results in an error score of 2.612. indicating inaccuracies introduced during the interpolation process.

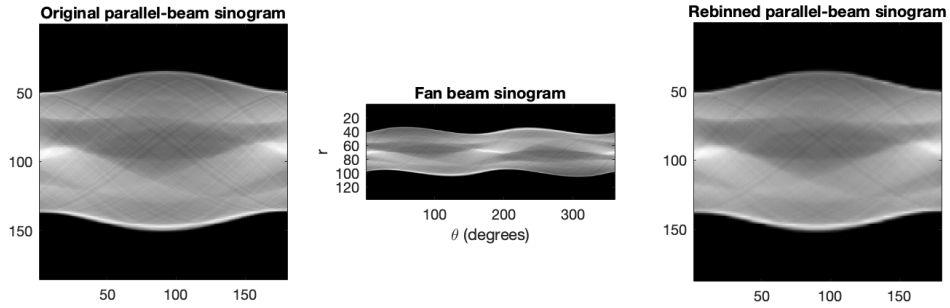

Figure 4: Original parallel-beam sinogram (left), rebinned fan-beam sinogram (middle), and rebinned parallel-beam sinogram (right)

In practical scenarios, while rebinning presents a viable solution, a shift in coordinate systems necessitating interpolation can introduce inaccuracies. Consequently, rebinning may not be the optimal solution. Alternatively, developing a dedicated reconstruction algorithm for fan beam projections can yield more accurate results, making it the preferred method.

2.2 The filter-backproject (FBP) approach for 360° scans

The fan beam FBP has an equivalent counterpart to the parallel beam FBP, enabling us to analytically reconstruct fan beam projection images. Firstly, we start by rewriting the parallel-ray FBP formula for the case of 360° rotation.

$$f(x,y) = \frac{1}{2}\int_0^{2\pi}\int p_\phi(r)\; h_*(x\cos\phi(s.\beta) + y\sin\phi(s.\beta) - r)\, dr\, d\phi \tag{5}$$

Using the change of variable: $r = r(s)$ and $\phi = \phi(s,\beta)$, the determinant of the change of variable is: $J(s) = |D_{so}cos\gamma(s) - r_{off}sin\gamma(s)||\dot{\gamma(s)}|$; while $h_*(.)$ denotes the ramp filter. Substituting the Jabobian J(s) into equation (5) the following is obtained:

$$f(x,y) = \frac{1}{2}\int_0^{2\pi}\int w_{2\pi}(x,y;\phi(s,\beta))\; p(s,\beta)\; h_*(x\cos\phi(s.\beta) + y\sin\phi(s.\beta) - r(s))J(s)\, ds\, d\beta \tag{6}$$

Given $x_\beta = x\cos\beta + y\sin\beta$ and $y_\beta = -x\sin\beta + y\cos\beta$ and using trigonometric identities, the following relationships are obtained:

$$L_\beta(x,y) = \sqrt{(D_{s0} - y_\beta)^2 + (x_\beta - r_{off})^2} \tag{7}$$

$$\gamma_\beta(x,y) = \arctan\left(\frac{x_\beta - r_{off}}{D_{s0} - y_\beta}\right) \tag{8}$$

$$s_\beta(x,y) = \begin{cases} D_{sd}\gamma_\beta(x,y), & \text{if } D_{fs} = 0 \text{ (equiangular)} \\ D_{sd}\tan\gamma_\beta(x,y), & \text{if } D_{fs} = \infty \text{ (equidistant)} \end{cases} \tag{9}$$

Substituting equation (7),(8) and (9) into (6) and applying some scaling property and algebraic manipulation, the formula for fan beam reconstruction is simplified as follows:

$$f(x,y) = \int_0^{2\pi} \frac{1}{W_2^2(x,y,\beta)L_\beta^2(x,y)}\left[\int p(s,\beta)\frac{w_{2\pi(s,\beta)J()s}}{W_1^2(s)} g_*(s_\beta(x,y) - s)ds\right] d\beta \tag{10}$$

W_1 and W_2 represent weighting functions, and $g_*(s)$ denotes the ramp filter. The weight function and filter differ for equiangular and equidistant cases, and their detailed explanations will be presented in subsequent subsections. In essence, Equation (10) can be interpreted as the summation of projection images that is weighted with W_1 and filtered along the detector axis s, followed by a secondary weighting with W_2 and summation across all projection angles β. With this mathematical foundation, the subsequent sections will delve into a comprehensive explanation of the fan beam "weighted" FBP formula.

Outline of the FBP formula:

- Step 1. Compute weighted projections for each β.

$$\overline{p}(s,\beta) = p(s,\beta)\frac{w_{2\pi}(s,\beta)J(s)}{W_1^2(s)} \tag{11}$$

- Step 2. Filter those weighted projections (along s) for each β using the modified ramp filter

$$\overline{p}(s,\beta) = \overline{p}(s,\beta) * g_s(s) \tag{12}$$

- Step 3. Perform a weighted backprojection of those filtered projections:

$$f(x,y) = \int_0^{2\pi} \frac{1}{W_2^2(x,y,\beta)L_\beta^2(x,y)} \overline{p}(s_\beta(x,y),\beta)d\beta \tag{13}$$

In general, the algorithm is fairly similar to parallel beam FBP except for the weighting function that is applied to the forward projection and backprojection, and a difference in the ramp filter for the equiangular case.

2.2.1 Equiangular case

This correspond to the case where an arc/ curved detector is used. Given we have:

$$\sin(\gamma_\beta(x,y) - \gamma(s)) = W_2 W_0(s_\beta(x,y) - s) \tag{14}$$

Substituting equation (1), (8) and (9) into (14), the forward projection weighting, filter and backprojection weighting are given as:

i. Projection weighting ratio in equation (11):

$$\frac{J(s)}{W_1^2(s)} = J(s) = \frac{1}{D_{sd}}|D_{so}\cos\frac{s}{D_{sd}} - r_{off}\sin\frac{s}{D_{sd}} \approx \frac{D_{so}}{D_{sd}}\cos\frac{s}{D_{sd}} \tag{15}$$

ii. Modified ramp filter in equation (12), where $\triangle_s$ denotes the detector element spacing:

$$h[n] = \begin{cases} \frac{1}{4\triangle_s^2}, & n = 0 \\ 0, & n \text{ even} \\ \frac{-1}{[\pi D_{sd}\sin(n\triangle_s/D_{sd})]^2}, & n \text{ odd} \end{cases} \tag{16}$$

iii. Backprojection weighting ratio in equation (13):

$$\frac{1}{W_2^2 L_\beta^2(x,y)} = \frac{D_{sd}^2}{L_\beta^2(x,y)} = \frac{D_{sd}^2}{(D_{s0} - y_\beta)^2 + (x_\beta - r_{off})^2} \tag{17}$$

2.2.2 Equidistant case

This correspond to the case where a flat detector is used and the forward projection weighting, filter and backprojection weighting are:

i. Projection weighting ratio in equation (11):

$$w_{2\pi}(s,\beta)\frac{J(s)}{W_1^2(s)} = \frac{w_{2\pi}(s,\beta)}{D_{sd}}|D_{so}\cos\gamma(s) - r_{off}\sin\gamma(s) \approx w_{2\pi}(s,\beta)\frac{D_{so}}{\sqrt{D_{sd}^2 + s^2}} \tag{18}$$

ii. Ordinary ramp filter in used in equation (12):

$$h[n] = \begin{cases} 1, & n = 0 \\ 0, & n \text{ even} \\ \frac{-1}{(\pi n/2)^2}, & n \text{ odd} \end{cases} \tag{19}$$

iii. Backprojection weighting ratio in equation (13):

$$\frac{1}{W_2^2 L_\beta^2(x,y)} = \frac{D_{sd}^2}{(\cos\gamma_\beta(x,y) L_\beta(x,y))^2} = \frac{D_{sd}^2}{(D_{s0} - y_\beta)^2} \tag{20}$$

Using the same geometrical setup from section 2 to obtain the forward projection for the equidistant case, the resulting weighted sinogram after applying the weighting ratio from equation (18) is *figure 5 (left image)*. If filtering from step 2 FBP algorithm is not applied, the reconstructed image is *figure 5 (center image)*. Otherwise, the reconstructed image is *figure 4 (right image)*.

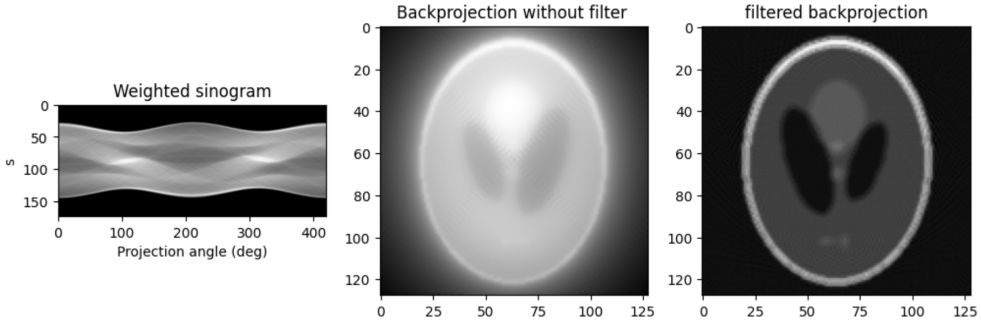

Figure 5: Weighted singoram (left), Unfiltered sinogram (center), and Filtered sinogram (right)

2.3 FBP for short scans

Fan beam CT setup that performs scanning of the object with less than a full rotation is known as a short scan. The preceding sections assume a full 360° rotation. Every ray is sampled exactly twice when a 360° scanning is used. In a short scan setting, 2 ray integrals represented by fan-beam angles (β_1, γ_1) and (β_2, γ_2) are identical if $\gamma_1 = -\gamma_2$ and $\beta_2 = \beta_1 + 2\gamma_1 + \pi$ [2]. Then, a short scan setting uses $(\beta_{max} = \pi + 2\gamma_{max})$ so that every point in the equivalent parallel beam sinogram is sampled at least once but some points are sampled twice. To account for the undersampled sinogram, an appropriate weighting function known as **Parker weighting** is used to replace the regular weighting function in equation (11). The weighting function is:

$$w_{2\pi}(s,\beta) = \begin{cases} q(\frac{\beta}{2(\gamma_{max}-\gamma)}), & 0 \leqslant \beta \leqslant 2(\gamma_{max}-\gamma) \\ 1, & 2(\gamma_{max}-\gamma) < \beta < \pi - 2\gamma \\ q(\frac{\pi+2\gamma_{max}-\beta}{2(\gamma_{max}+\gamma)}), & \pi - 2\gamma \leqslant \beta \leqslant \pi + 2\gamma_{max} \end{cases} \tag{21}$$

where $q(x) = \sin^2(\frac{\pi}{2}x)$ and fan sinogram data where $0 \leqslant \beta \leqslant 2(\gamma_{max} - \gamma)$ and $\pi - 2\gamma \leqslant \beta \leqslant \pi + 2\gamma_{max}$ are identical rays.

Similar to the geometrical setup from section 1, except (i) 180 projections; (ii) arc/γ = 128, *figure 6 (left)* shows the resulting short sinogram. It can be seen that certain areas of the sinogram are sampled twice and this causes the asymmetry in the short sinogram which necessitates the use of Parker's weighting. The Parker weighted sinogram is shown in *figure 6 (center)* and it can be seen that the sinogram now looks symmetrical. Finally, *figure 6 (right)* shows the reconstructed sinogram that is weighted using Parker's weighting.

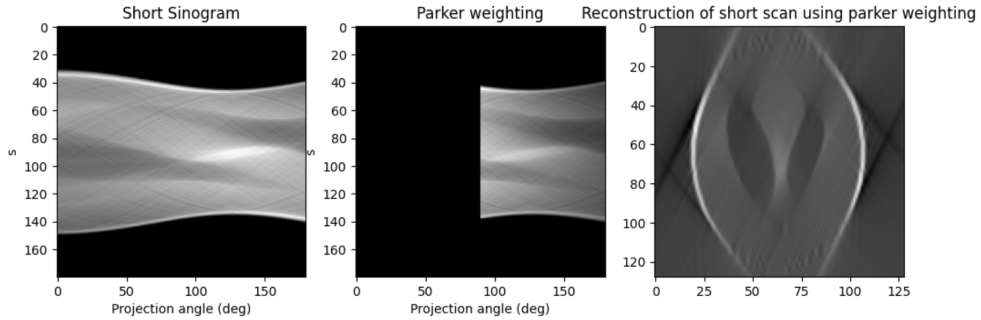

Figure 6: Short sinogram (left), Short sinogram with Parker's weighting (center), Reconstructed short sinogram with Parker's weighting (right)

2.4 The backproject-filter (BPF) approach

Similar to parallel beam reconstruction, it is also possible to use the BPF approach for fan-beam tomography. Given the fan beam projections from equation (3), for $\beta \in [0, \beta_{max}]$ and weighting function $w_{BPF}(s, \beta)$, the weighted backprojection is

$$b(x, y) == \int_{-s_{max}}^{s_{max}} \int_{0}^{\beta_{max}} \delta(x \cos\phi(s.\beta) + y \sin\phi(s.\beta) - r(s)) p(s, \beta) w_{BPF}(s, \beta)\, ds\, d\beta \tag{22}$$

The BPF formula in equation (22) can be outlined step by step as follows: [3]:

- Step 1. Backproject the projection measurements
- Step 2. Take the two-dimensional FFT of the backprojection image.
- Step 3. Apply the ramp filter to the Fourier transformed image.
- Step 4. Take the inverse two-dimensional FFT of the filtered image to obtain the reconstruction

Again using the geometrical setup from section 2, *figure 7* shows the resulting reconstructed image using the BPF approach. Even though the phantom is discernible from the reconstruction, the quality of the image lacks that of the FBP method as the colour contrast is noticeably poorer.

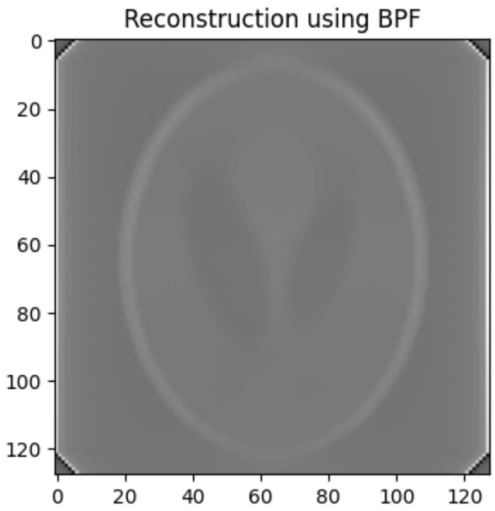

Figure 7: Reconstruction using backprojection filter

3 3D CONE-BEAM RECONSTRUCTION

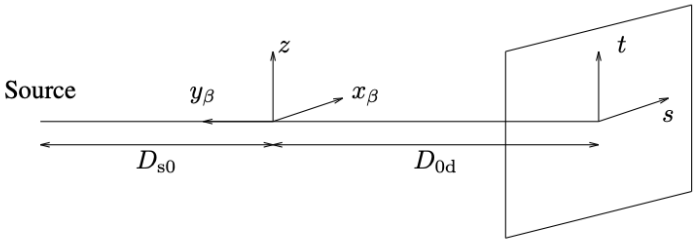

Figure 8: Cone beam geometry, source: [1]

In X-ray CT, acquiring 3D projections of objects is achievable through cone beam scanning, akin to the fan beam geometry discussed in Section 2. However, in this case, the X-ray detector is two-dimensional instead of one-dimensional. Consequently, a distinct algorithm is necessary to reconstruct the 3D sinogram data. This section specifically delves into the scenario of a 360° circular X-ray source trajectory, known as an axial scan, although alternative acquisition methods also exist. The algorithm employed for reconstructing the resulting sinogram is recognized as the **Feldkamp cone beam algorithm** or **FDK approach**. Remarkably, it shares many similarities with the FBP discussed in Section 2.

3.1 Equidistant case (flat detector)

(Figure 8) illustrates the geometry of a cone-beam flat detector. It is fairly similar to the 2D fan beam in terms of geometry and parameters with the exception of an extra parameter **t** to account for an extra dimension in the detector. (x_β, y_β) shown here is the rotated coordinates that is defined as $x_\beta = x\cos\beta + y\sin\beta$ and $y_\beta = -x\sin\beta + y\cos\beta$. In addition, β denotes the angle of the source point counter-clockwise from the y axis. Hence, the cone-beam line-integral projections formula can be written as:

$$p(s,t;\beta) = \int_{L(s,t;\beta)} f(x,y,z)\,dl \tag{23}$$

Given a 3d test phantom f(x,y,z) of size of 64 along all dimension, *figure 9 (top)* shows the test phantom at slice 32 along dimension 0, 1 and 2. Applying the forward projection using the geometrical setup for equidistant case - (i) 180 projections; (ii) arc/ γ = 360; (iii) D_{so} = 12800; (iv) D_{od} = 128; (v) offset = 0; (vi) Size of the detector/ [s,t] = [120,120]; (vii) Sino and volume spacing = 1 (unit spacing); (viii) Joseph projection method, *figure 9 (bottom)* depicts the forward projection along dimension 0,1 and 2.

The same ramp filter from equation (19) is applied to the (weighted) measurements from each row of the detector. After that, the 3D cone-beam backprojection is performed using the image-domain weighting given in equation (20). In summary, the steps of the FDK algorithm for the equidistant case are:

Outline of the FDK approach:

- Step 1. Compute weighted projections using the projection weighting w1 given below.

$$\overline{p}(s,t;\beta) = w_1(s,t)p(s,t;\beta), \qquad w_1(s,t) = \frac{D_{so}}{\sqrt{D_{sd}^2 + s^2 + t^2}} \tag{24}$$

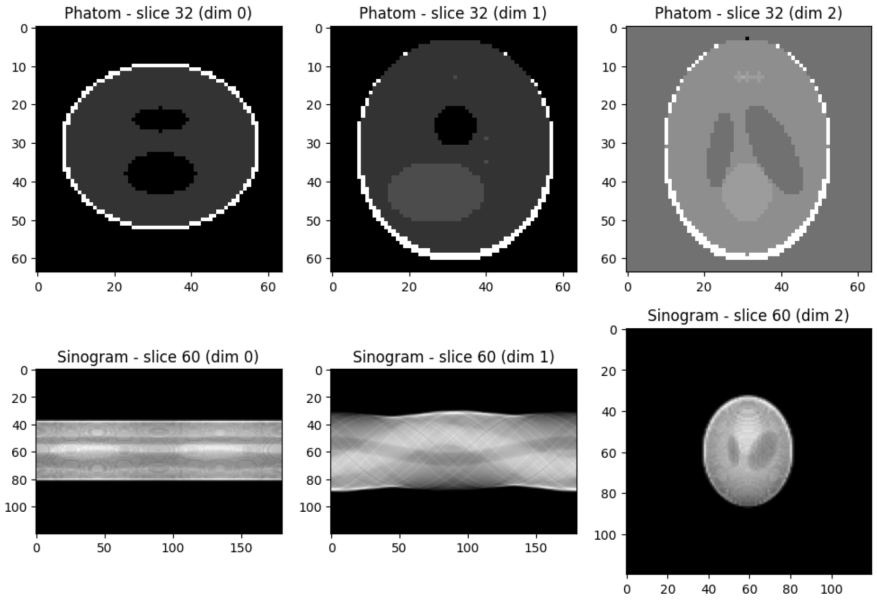

Figure 9: Top images show the phantom along different dimension at slice 32, bottom images show the sinogram along different dimensions at slice 60

- Step 2. Filter those projections along each row of the detector as if it were part of a 2D fan-beam acquisition using the ordinary ramp filter $h_*(s)$ from equation (19)

$$\overline{p}(s,t;\beta) = \overline{p}(s,t;\beta) * h_*(s) \tag{25}$$

- Step 3. Perform weighted cone-beam backprojection of those filtered projections using the weighted function w2, s_β, and t_β.

$$\hat{f}(x,y,z) = \frac{1}{2}\int_0^{2\pi} w_2(x,y,\beta)\overline{p}(s_\beta(x,y), t_\beta(x,y,z);\beta), d\beta \tag{26}$$

where

$$w_2(x,y,\beta) = \frac{D_{sd}^2}{(D_{so} - y_\beta)^2} \qquad s_\beta(x,y) = \frac{D_{sd}}{D_{so} - y_\beta}x_\beta \qquad t_\beta(x,y,z) = \frac{D_{sd}}{D_{so} - y_\beta}z \tag{27}$$

The reconstruction using the FDK approach above along each dimensions can be seen in *figure 10* below. Strangely only the image on dimension 0 is properly reconstructed but they are not on dimension 1 and 2.

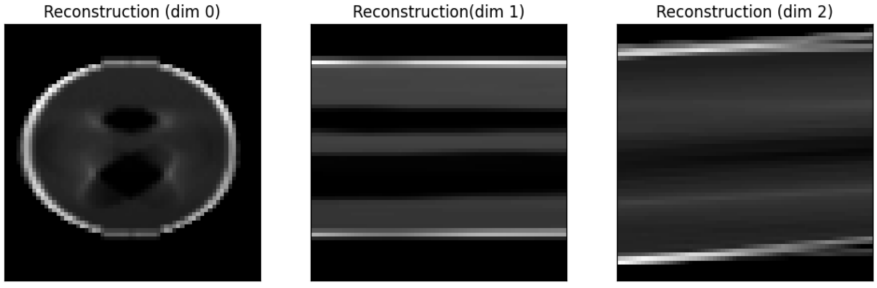

Figure 10: Reconstructions along different dimensions using the FDK algorithm

Using the backprojection method (applyAdjoint) from the Elsa library, *figure 11* shows the well reconstructed test phantom along all 3 dimension.

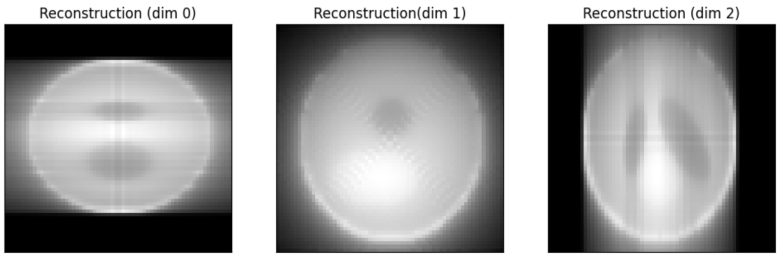

Figure 11: Reconstructions along different dimensions using elsa

3.2 Equiangular case (3rd generation multi-slice CT)

In a 3rd-generation multi-slice CT scanner, the FDK algorithm follows the same general steps as the equidistant method discussed earlier. Similar to fan-beam tomography in the equiangular case, the distinctions lie in the projection weighing, filtering, and backprojection weighting utilized.

i. Replace the 1D weighting equation (24) by

$$w_1(s,t) = \frac{D_{so}}{\sqrt{D_{sd}^2 + t^2}} \cos\left(\frac{s}{D_{sd}}\right) \tag{28}$$

ii. Replace the filter in equation (25) with the modified ramp filter in equation (16).

iii. In equation (27), weighting ratio $w_2(x,y,\beta)$ is replaced with equation (17); $s_\beta(x,y)$ is replaced with (9) and $t_\beta(x,y,z)$ remains unchanged.

3.3 Extensions of cone beam CT methods

3.3.1 Helical scan

The previous section on 3D cone beam CT assumes the use of the axial scanning method. In axial scanning, the patient or object to be imaged lies on the gantry while the X-ray source detector moves in a circular or elliptical path around the patient. At each angular position, a set of X-ray measurements is acquired and the object moves to a new position after each rotation. A more recent approach, known as the helical scanning method, involves continuous rotation of the X-ray source and detectors while the patient or imaged object moves through the gantry. This results in continuous data acquisition, creating a helical or spiral dataset. The helical scanning method offers a shorter acquisition time and is more commonly used today. Importantly, a filtered backprojection (FBP) reconstruction is applicable to the helical source trajectory, allowing for theoretically exact reconstruction.

3.3.2 Cone-parallel rebinning

Following a concept similar to that discussed in section 2.1, cone beam projections can be rebinned to parallel beam projections that can lead to FBP method with simplified computation and reduced noise that is applicable to both axial and helical scanning trajectories. This approach works by converting fans for each detector row into cone-parallel rays. The parallel beam projections are expressed in terms of cone-beam projections using the following relationship:

$$p_{CP}(r,\phi;t) = p(s,t;\beta)|_{s=s(r),\beta=\beta(r,\phi)} = p(\gamma^{-1}(\arcsin r/D_{so}, t; \phi - \arcsin r/D_{so})) \tag{29}$$

4 RETROSPECTIVE

Recognizing the complexity of the subject matter during my first read through the topic, I anticipated challenges for audiences unfamiliar with CT concepts. To enhance accessibility, I tailored the session for those at a beginner to intermediate level. This approach involved a gradual introduction with ample illustrations, particularly easing into intricate topics like the reconstruction algorithms. Given the reconstruction algorithms used emphasis a profound grasp of underlying geometry, I dedicated substantial time to explain geometry in detailed. This served as a foundational element for subsequent discussions on forward and backprojection. To simplify these concepts, I strived to use straightforward terms to explain intricate formulas, i.e, the forward and backprojection formula as I acknowledge potential difficulties in comprehending formal definitions and formulas.

Overall, I am satisfied with the content of the presentation as I believe it is difficult to further simplify the topic without shining light on the mathematical nuances of the algorithms which seem to be the focus of the author. However, I believe that my communication especially in certain areas can be further improve as constant worrying about time constraints may have led to a rushed delivery. This impacts the clarity of certain explanations which may be delivered in a better way to enhance understanding. In retrospect, I think I might need to refine my communication especially in the later part of the presentation.

In evaluating the demonstration segment, I am generally content with the implementation of the fan beam tomography demo scripts. However, one point of regret is the imperfect functionality of the cone beam reconstruction, resulting in the reconstruction of only the image on the first dimension. I primarily referred to J.Fessler's implementation, adapting my FDK algorithm accordingly to align with the input parameters used by the Elsa library. While adjusting the computation steps and variable manipulation to closely mirror J.Fessler's implementation, there remains a limitation in achieving perfect cone beam reconstruction. Despite this, I also attempted reconstruction using the 3D sinogram with Elsa's algorithm, aiming to provide the audience with a sense of a plausible reconstruction. Similarly, the rebinning method yielded undesirable results, prompting me to illustrate using the built-in Matlab library to convey the intended outcome to the audience.

REFERENCES

[1] J. Fessler. Image reconstruction: Algorithms and analysis. *Book draft*, 20:3.28, 2023.

[2] A. Kak and M Slaney. Principles of computerized tomographic imaging. *Book*, pages 49–107, 1988.

[3] G. L. Zeng G. T. Gullberg. Backprojection filtering for variable orbit fan-beam tomography. *IEEE TRANSACTIONS ON NUCLEAR SCIENCE*, 42, 1995.